Supplementary information

Co-condensation and co-evaporation of levoglucosan onto and from deliquesced ammonium sulfate particles – influence of relative humidity, particle mass and size, and presence of a surfactant

Jian Xu[1, a, *], Junteng Wu[1,2,*], Mayur Gajanan Sapkal[3], Jim Grisillon[1], Shravan Deshmukh[4], Brice Temime Roussel[1], Julien Kammer[1], Nicolas Brun[1], Fabien Robert-Peillard[1], Beiping Luo[3], Judith Kleinheins[3], Silvia Henning[4], Bénédicte Picquet-Varrault[5], Edouard Pangui[5], Mathieu Cazaunau[5], Zamin A. Kanji [3], Claudia Marcolli[3], Anne Monod[1]

[1]Aix Marseille Université, CNRS, LCE, Marseille, France

[2]Université Clermont Auvergne, CNRS, OPGC, LaMP, F-63000 Clermont Ferrand, France

[3]Institute for Atmospheric and Climate Science, ETH Zürich, Zürich, Switzerland

[4]Leibniz Institute for Tropospheric Research (TROPOS), 04318 Leipzig, Germany

[5]Univ Paris Est Creteil and Université de Paris Cité, CNRS, LISA, F-94010 Créteil, France

[a]Now at Department of Chemistry, University of Oslo, Oslo, Norway.

* Two first authors, as both authors contributed equally to this work

Correspondence to: Jian Xu (jianxuu@gmail.com), Junteng Wu (junteng.wu@uca.fr) and Anne Monod (anne.monod@univ-amu.fr)

SI-1: Pre-experiments of generation of particles containing AS and SDS

Prior the CESAM campaign, a series of pre-experiments was performed to test the generation of monodispersed particles containing AS and SDS at various sizes (Fig. S1). The goal was to obtain monodispersed particles containing AS and SDS at comparable concentrations. An aqueous solution of AS and SDS was atomized into polydisperse particles which were then dried and size-selected using the

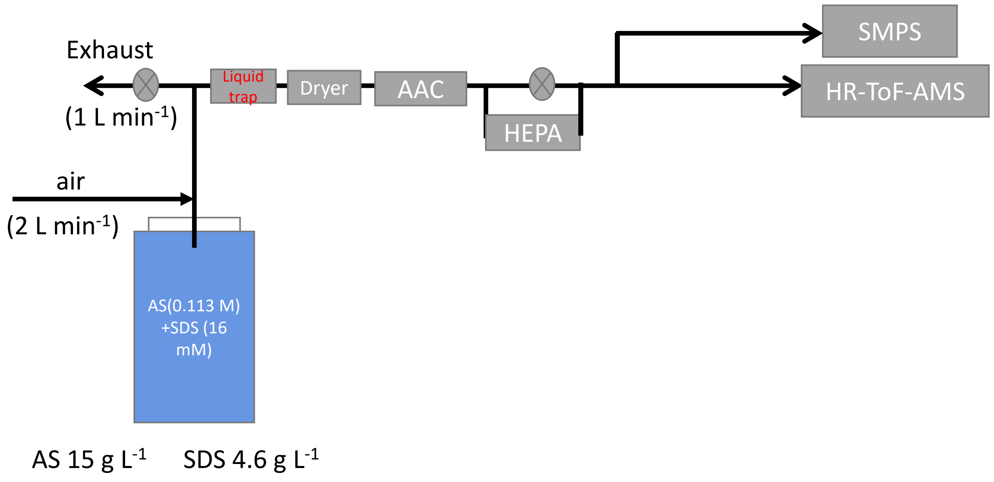

Figure S1 : Experimental setup to test the generation of particles containing AS and SDS instruments described in the main text (section 2.4). Their size and chemical composition were monitored on-line using an SMPS and the AMS described in the main text (section 2.5).

The SDS concentration in the solution was set to 16 mM, which is higher than its CMC. In pure water, the CMC of SDS is 8.2 mM at 25°C (Markarian et al., 2005), but it can decrease down to 1.2 mM in the presence of metallic cations (Moroi et al., 1974) and 0.5 mM in the presence of salts (Umlong and Ismail, 2007). In the present work, the chosen SDS concentration was still much lower than its water solubility (1.4 M, (Lee et al., 2021)). It was a compromise between the high concentrations required to coat as much as possible the surface of the generated particles and the low concentrations needed to limit the foam formed into the system. Additionally, a very large liquid trap consisting of a 16 L glassware vessel was needed prior the drier (in red in Fig. S1). The results showed that the particles obtained using this experimental setup were composed of AS and SDS at a constant mass ratio of ~1:1, regardless of the mobility diameter: 90, 100, 200, 300 nm or polydisperse.

SI-2: Details on experiments 4a and 4b

S2-1 AMS-derived SDS concentration in the particle

The SDS concentration is derived from AMS measurement using Eq. S1, where $c_{SDS,j}^{air}$ is the concentration of SDS at time j (in µmol m^{-3}), $c_{org.,j}^{air}$ is the total organic mass concentration measured by the AMS at time j, $c_{levo.,j}^{air}$ is the levoglucosan mass concentration measured by the AMS at time j, and M_{frag} is the molar mass of the organic fragment of SDS, i.e. the alkyl chain $C_{12}H_{25}$ without the sulfate moiety (at m/z 168.19 see text, section 2.5.1). Note that because of the presence of impurities (Wu et al. 2022), the obtained SDS concentration is a slight overestimation of the real SDS concentration.

$$c_{SDS,j}^{air} = \frac{c_{org.,j}^{air} - c_{levo.,j}^{air}}{M_{frag}} . \qquad \text{Eq. S1}$$

The obtained SDS concentration in the air is then converted into a concentration in the particle $c_{SDS,j}^{AMS}$ at time j with Eq. S2, where $n_{j,part}$ is the particle number concentration measured by the SMPS at time j, and $V_{part,j} = \frac{\pi}{6} {D_{ve,j}}^3$ is the volume of the wet particle obtained from the volume equivalent diameter $D_{ve,j}$ measured by the SMPS at time j. Note that the volume of the wet particle is underestimated due to the lower RH% encountered in the SMPS compared to the CESAM chamber, especially at high RH.

$$c_{SDS,j}^{AMS} = \frac{c_{SDS,j}^{air}}{n_{j,part} V_{part,j}} = \frac{c_{SDS,j}^{air}}{n_{j,part} \frac{\pi}{6} {D_{ve,j}}^3} . \qquad \text{Eq. S2}$$

S2-2 Filter-derived SDS concentration in the particle

Particles were collected on a 47 mm quartz fibre filter during each experiment, starting when particles were introduced in CESAM, and ending at the end of the experiment. The targeted collection flow rate was 2.3 L.min^{-1}, but this varied depending on the total flow extracted from CESAM, resulting in an average value of 2.5 (± 2.3) and 0.89 (± 0.77) L.min^{-1} for Exp 4a and 4b, respectively. After collection, the filters were immediately covered with aluminium foil and stored in Petri slides at -20 °C prior to analysis. Then, a simplified version of the methodology for surfactants quantification in aerosols proposed by (Grisillon et al. 2026) was used to measure the SDS concentration. The filter was extracted in 20 mL of ultrapure water. The resulting solution was subjected to three cycles of 30 s of hand shaking and 30 s of ultrasonic bath. The mixture was stirred overnight using a reciprocating shaker (180 rpm). The next morning, the same three cycles of shaking and ultrasonication were applied to the mixture. The solution was then filtered using a home-made polyethylene filter (pre-cleaned with 50 mL of ultrapure water; see (Grisillon et al. 2026) for more details). After filtration, 2 mL of methanol were filtered to recover all surfactants that could be adsorbed on the filter membrane. These 2 mL of methanol were added to the 20 mL of filtrate, and the solution was completed to 50 mL.

SDS was then preconcentrated using a solid phase extraction step with Oasis® HLB (hydrophilic-lipophilic balanced) sorbents. The conditioning was performed with 10 mL of methanol, followed by 10 mL of a 0.1% solution of NH_3 in MeOH, and 5 mL of a 2 mM HCl aqueous solution. The 50 mL solution obtained after the extraction step, acidified with 10 µL of pure hydrochloric acid, was percolated through the cartridge. 5 mL of water was then added, followed by 1 min of drying under vacuum. The elutions were performed as follows: 1) 4 mL of methanol, and 2) 2 mL of the 0.1% solution of NH_3 in MeOH. The eluates were gathered in a 60 mL glass tube, and the solvents were evaporated at 45 °C under a gentle N_2 flux.

10 mL of ultrapure water were added into the glass tube, and a test designed for strong anionic surfactants was performed (Grisillon et al. 2026). 200 µL of 1 M phosphate buffer solution at pH 2.3, 100 µL of ortho-toluidine blue (TBO) solution (0.1 g.L^{-1} in ultrapure water) and 2 mL of chloroform were added. The resulting mixture was shaken vigorously for 30 s to perform a liquid-liquid extraction of the surfactant-dye (SDS-TBO) complex into the chloroform phase. After 15 min of rest, the aqueous and organic phases were completely separated. 1 mL of the chloroform phase was extracted and analysed with a spectrophotometer (Jasco V-670). A peak corresponding to the TBO is visible on the spectrum, which height is proportional to the TBO – and thus to the SDS – concentration in the chloroform. More details on the calibration can be found in (Grisillon et al. 2026). This measurement provides the total amount of SDS collected on the filters n_{SDS}^{tot}.

Blanks were performed with filters collected during the CESAM experiments involving only AS and levoglucosan (Exp 3g and 3h). The measured concentrations of surfactants in these samples were below the limit of detection, proving that only SDS was detected by this technique in Exp 4a and 4b, and not levoglucosan or AS.

To obtain the SDS concentration in the particle, the total amount of SDS is first divided by the number of particles collected N, given by Eq. S3, where $n_{i,part}$ is the number concentration of particles at time i measured by the SMPS, Δt is the measurement time step of the SMPS, equal to 2.5 min, and F_i is the flow rate of collection on the filter at time i, calculated as the difference between the total flow and the sum of flows of all instruments.

$$N = \sum_i n_{i,part} \Delta t F_i \, . \qquad \text{Eq. S3}$$

This gives the amount of SDS molecules in each particle, with the assumption that all particles are internally mixed and that this number does not vary with time during the experiment. The SDS concentration in the particle at time j $c_{SDS,j}^{filter}$ is further obtained by Eq. S4, where $V_{part,j} = \frac{\pi}{6} {D_{ve,j}}^3$ is the volume of the wet particle obtained from the volume equivalent diameter $D_{ve,j}$ measured by the SMPS, at time j, and n_{SDS}^{tot} is the total amount of SDS collected on each filter.

$$c_{SDS,j}^{filter} = \frac{n_{SDS}^{tot}}{NV_{part,j}} = \frac{n_{SDS}^{tot}}{N\frac{\pi}{6}D_{ve,j}{}^{3}} . \qquad \text{Eq. S4}$$

$c_{SDS,j}^{filter}$ and $c_{SDS,j}^{AMS}$ were calculated at different times during Exp. 4a and 4b and are compared in Table 2 in the column "SDS total concentration".

S2-3 Calculation of SDS surface coverage

The surface coverage is calculated as proposed by (Jacobs et al. 2024). The partitioning of SDS is described with a Langmuir isotherm (Langmuir 1918). The relationship between the surface excess Γ_{SDS} (analogous to the surface concentration) and the bulk concentration c_{SDS}^{bulk} is shown in Eq. S5, where Γ_{SDS}^{max} is the maximum surface excess (i.e. the maximum surface concentration) and K_{ads} is the adsorption equilibrium constant. Then, the surface coverage θ stands for the SDS surface excess divided by the maximum SDS surface excess. Values for Γ_{SDS}^{max} and K_{ads} are 11.3 10^{-6} mol m^{-2} and 300 L mol^{-1}, respectively, and were taken from (AlSoufi et al., 2012).

$$\theta = \frac{\Gamma_{SDS}}{\Gamma_{SDS}^{max}} = \frac{K_{ads}c_{SDS}^{bulk}}{1+K_{ads}c_{SDS}^{bulk}} . \qquad \text{Eq. S5}$$

Therefore, c_{SDS}^{bulk} must be known to calculate the surface coverage θ. However, AMS and filter data only provide total concentrations of SDS in the particles. Therefore, c_{SDS}^{bulk} must be calculated thanks to a partitioning equation, or mass conservation. It is assumed that SDS only partitions between the surface and the bulk, but no micelle is formed. Then, the total concentration is the sum of the bulk concentration and the surface concentration multiplied by a scaling factor that turns the surface concentration into a volumetric concentration. Eq. S6 describes this partitioning, with $\mathcal{A}$ and $\mathcal{V}$ the surface area and volume of the particle, respectively.

$$c_{SDS}^{tot} = c_{SDS}^{bulk} + \Gamma_{SDS}\frac{\mathcal{A}}{\mathcal{V}} = c_{SDS}^{bulk} + \Gamma_{SDS}^{max}\frac{K_{ads}c_{SDS}^{bulk}}{1+K_{ads}c_{SDS}^{bulk}}\frac{\mathcal{A}}{\mathcal{V}} . \qquad \text{Eq. S6}$$

c_{SDS}^{bulk} was calculated by solving Eq. S6, and then injected into Eq. S5 to calculate the surface coverage θ. The values of the surface coverage obtained at the different times are indicated in Table 2.

S2-4 Calculation of surface tension

The surface tension of the particle is calculated using Eq. S8, with $\sigma_w = 0.0720$ N m^{-1}, $R = 8.314$ $JK^{-1}mol^{-1}$, $T = 298$ K, and θ is calculated as described in the above section. $\sigma = 0.0345\ N\ m^{-1}$ corresponds to the minimum surface tension of SDS in aqueous solutions (Al-Soufi et al. 2012).

$$\sigma = \max(\sigma_w + \Gamma_{SDS}^{max}RT\ ln(1-\theta), 0.0345). \qquad \text{Eq. S8}$$

SI-3 : details on the correction of MPSS data

Because of technical issues with the dryer, the RH sensor integrated into the sheath flow of the MPSS indicated values ranging from below 15 to 50%, depending on the RH in CESAM. It was thus necessary to adopt a methodology of particle size correction to obtain dry particle size and mass concentrations, as described below.

S3-1 Water uptake of ammonium sulfate and levoglucosan mixed particles in the literature

The drying process involves dehumidifying the deliquesced particles. Lei et al. (2018) experimentally investigated the hygroscopic growth of AS and mixtures of AS/levoglucosan aerosols using an H-TDMA using various Levo/sulfate ratios ($f_{o/s}$) and RH covering a large range, from 15% to 90% (Fig SI3-1).

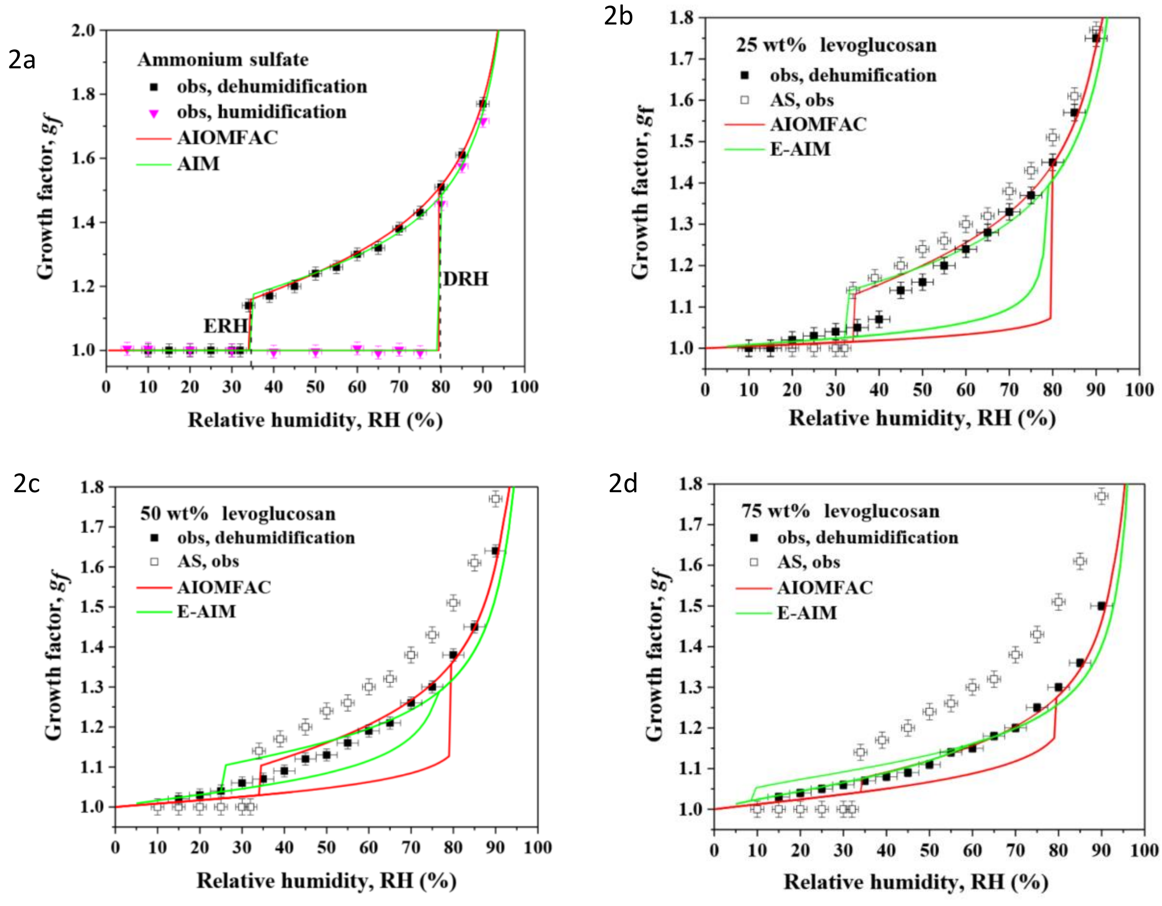

Figure S2. Four figures are reproduced from Lei et al., 2018, Atmospheric Chemistry and Physics, under the Creative Commons Attribution 4.0 License (CC BY 4.0) on selected dry particles at ***d**$_m$***=100** nm. Both experimental data (dots) and simulation data (continous lines) are shown for different compositions: (a) pure AS particles; (b), (c) and (d) mixed particles containing AS and levoglucosan : **25 wt%, 50 wt%** and **75 wt%** of levoglucosan respectively in the nebulisation solution.

Fig. S2-a shows that both simulations (AIOMFAC and E-AIM) agree with the experimental data for pure AS particles (Lei et al., 2018). Fig SI-31-b, c and d show the results obtained for mixed aerosols of ammonium sulfate and levoglucosan with increasing proportions of levoglucosan (in the nebulizing solution). The Figure clearly shows that above 25% of levoglucosan (in the nebulizing solution), the efflorescence RH is difficult to observe experimentally, and both models are not reliable when levoglucosan is present. We thus used the experimental data of (Lei et al., 2018) and their interpolations to perform the corrections of particle size to obtain dry particle size and mass concentrations from MPSS data in the present study.

S3-2 Comparison of the experimental conditions between this work and that of Lei et al., 2018

Because we used the experimental data by Lei et al. (2018) to perform the corrections, a comparison between our experimental conditions and those of Lei et al. (2018) is shown in Table S1

Table S1. Comparison of the conditions for AS/levo experiments.

	This work	Lei et al., 2018
Atomizer model	TSI-3076	MSP 1500
Solute total concentration	30 gL^{-1}	0.5 gL^{-1} (0.05 wt%)
wt% of levo in the nebulized solution	50	0, 25, 50 and 75
Levo/sulfate mass ratio ($f_{o/s}$)	0.1-2.4 (measured by AMS)	0-4.13 (in the nebulized solution)
Levo%	5-64	0-75
Dry size selection	73-190 nm	100 nm
RH	1.4-85% (MPSS DMA)	5-90% (DMA2 in the HTDMA)
Measurement type	Chamber (0.75-1.5 hour during particle introduction filling)	On-line (no chamber)

Table S1 shows that Lei et al., (2018) performed online measurements, while this study was performed in a chamber. Furthermore, a different atomizer model was used, and a much lower total solute concentration in the nebulized solution was used in the online study of Lei et al. (2018). Nevertheless, the organic mass ratio, the selected particle size and RH range are similar.

Although the experimental conditions are not exactly the same, the levo/sulfate ratios studied by Lei et al., 2018 (0-4.13) range over those of this work (0.2-2.4). Additionally, in Lei et al., 2018, the RH in the DMA2 of the HTDMA varied over a large range (5-90%) and can be compared to the RH range in the MPSS DMA (25-95% in non-dry experiments of the present study).

S3-3 Interpolation of growth factors of ammonium sulfate and levoglucosan mixed particles from the work of Lei et al., 2018

The experimental data provided by Lei et al. (2018) (Fig SI-3-2) were interpolated as follows:
1/ For RH: The data were interpolated by 1% RH step for each levoglucosan levoglucosan to sulfate ratio ($f_{o/s}$);
2/ For levoglucosan to sulfate ratio ($f_{o/s}$): the data were interpolated by 1% concentration step at each RH.
The results of interpolations are shown and compared to the original data in Fig. S3.

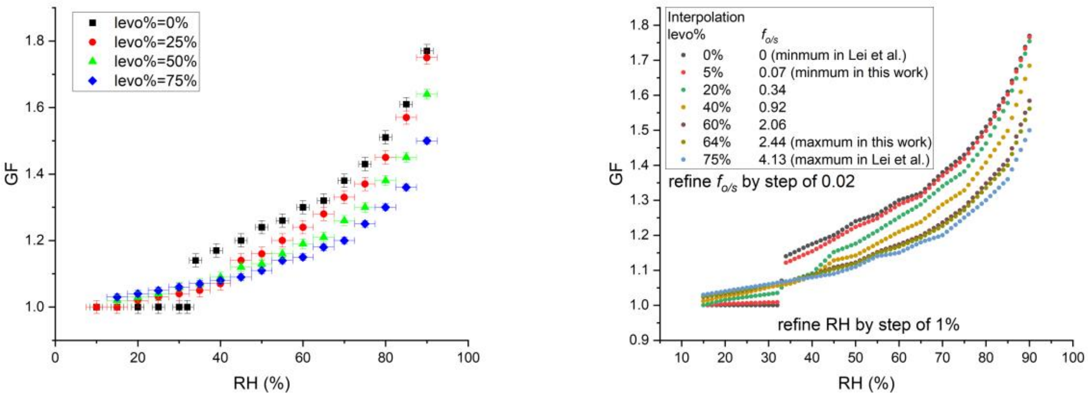

A. Original data of Lei et al., 2018

B. Interpolation data of Lei et al., 2018

Figure S3. Growth factor of particles as a function of RH% for mixed particles containing various levoglucosan/AS ratios. (A) original data from Lei et al. (2018); (B) Interpolation of growth factors from the work of Lei et al. (2018).

S3-4 growth factors $g\left(RH_{MPSS}, f_{o/s}\right)$ to correct the dry particle size and mass concentration obtained from the MPSS in the present study.

Based on the interpolation data shown in Fig SI-3-2, a two-dimensional matrix of growth factors $g\left(RH, f_{o/s}\right)$ was built as a function of RH and levogulcosan to sulfate ratio ($f_{o/s}$). By applying the RH measured in the sheath flow of the MPSS and $f_{o/s}$ measured by the AMS, $g\left(RH_{MPSS}, f_{o/s}\right)$ was then determined to obtain the dry particle size and dry mass concentration.

Applying this correction to all experiments performed under various RH conditions, Fig. S4 shows that the correction significantly impacted the size and mass concentrations of aerosol particles. When the MPSS sheath air was not completely dry, the discrepancy on the size reached more than 20% which is higher than the uncertainties of the instrument (10%, Wiedensohler et al., 2012), and the discrepancy on the total mass could reach 50%. These results showed that, to limit the bias below 10%, the RH inside the MPSS must be ≤ 15%.

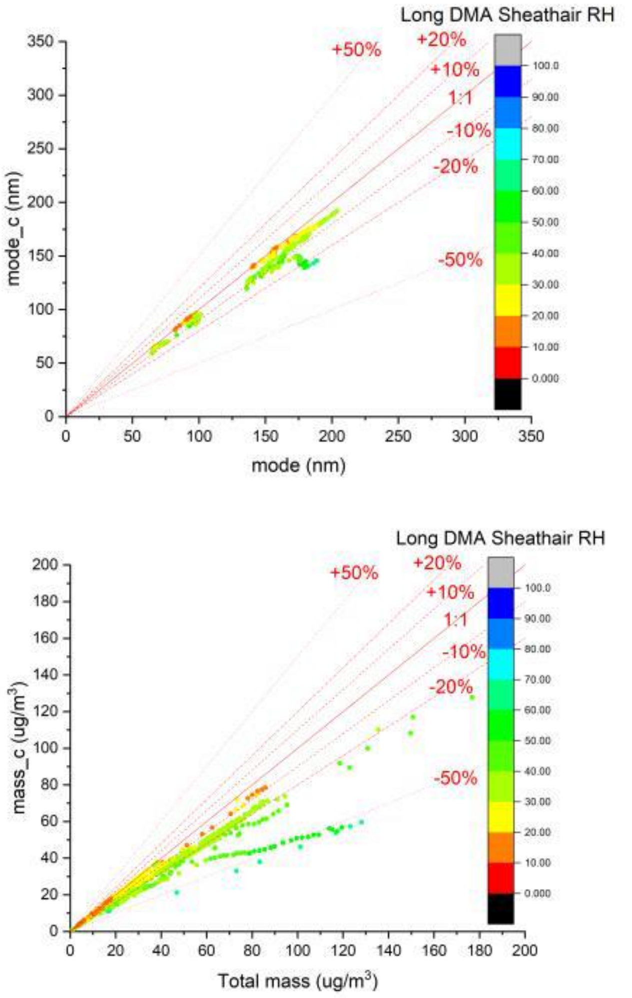

Figure S4. Comparison between uncorrected and corrected dry particle size (left) and mass (right)

SI-4: details on the construction of Figure 6

Pearson correlation coefficients in Fig. 6 were computed for all pairs of variables (k_{net}, RH, D_{ve}, m_{total}, $f_{o/s}$, and T) to evaluate their linear associations. In addition, the total organic mass concentration, m_{org}, was included in the analysis. Because of the likely different particle phase encountered under dry conditions (see text), the analysis was restricted to humid conditions and experiments conducted without SDS (experiments 3b–3h). The values of the extracted variables are listed in Table S2, they were taken as the average over a period of 40–60 minutes during the k_{net} fitting determination. The resulting correlation matrix (Fig. 6 in the text) provides a quantitative representation of the strength and direction of pairwise linear relationships within the dataset.

Table S2. Variables used for calculating the Pearson correlation coefficients

Exp	k_{net}	RH	D_{ve}	m_{org}	m_{total}	$f_{o/s}$	T
3b	4.36×10^{-5}	91.3	95.5	10.5	18.8	1.8	22.4
3c	3.36×10^{-5}	87.0	170.9	19.1	32.3	2.0	22.4
3d	-1.15×10^{-5}	97.8	167.2	16.0	26.3	2.08	23.1

3d	0.91×10^{-5}	99.8	169.2	12.1	19.9	2.13	23.2
3d	4.44×10^{-5}	96.0	168.6	8.4	14.6	1.99	23.4
3e	3.26×10^{-5}	87.1	171.7	25.7	41.2	2.38	23.8
3e	11.5×10^{-5}	76.0	159.7	13.7	24.5	1.76	23.7
3f	4.21×10^{-5}	88.9	175.3	23.0	37.5	2.1	24.4
3f	11.6×10^{-5}	82.8	171.1	13.5	24.8	1.6	24.5
3f	29.3×10^{-5}	65.1	144.1	1.6	8.5	0.5	24.8
3g	15.9×10^{-5}	87.1	93.0	5.3	11.2	1.2	23.8
3h	14.2×10^{-5}	90.7	78.6	5.4	10.0	1.6	24.4
3h	29.3×10^{-5}	82.3	75.0	2.1	5.8	0.7	24.5

Refences

Al-Soufi, Wajih, Lucas Piñeiro, et Mercedes Novo. 2012. « A model for monomer and micellar concentrations in surfactant solutions: Application to conductivity, NMR, diffusion, and surface tension data ». Journal of Colloid and Interface Science 370 (1): 102-10. https://doi.org/10.1016/j.jcis.2011.12.037.

Grisillon, Jim, Laurie Michel, Julien de Barry, et al. 2026. « Quantification of four classes of amphiphilic surfactants by solid phase extraction and spectrophotometric detection at nanomolar levels: environmental applications ». Talanta 297 (janvier): 128575. https://doi.org/10.1016/j.talanta.2025.128575.

Jacobs, Michael I., Madelyn N. Johnston, et Shahriar Mahmud. 2024. « Exploring How the Surface-Area-to-Volume Ratio Influences the Partitioning of Surfactants to the Air–Water Interface in Levitated Microdroplets ». The Journal of Physical Chemistry A 128 (46): 9986-97. https://doi.org/10.1021/acs.jpca.4c06210.

Langmuir, Irving. 1918. « The adsorption of gases on plane surfaces of glass, mica and platinum ». Journal of the American Chemical Society 40 (9): 1361-403. https://doi.org/10.1021/ja02242a004.

Lee, H. L., Cheng, Y. S., Yeh, K. L., and Lee, T.: A Novel Hydrate Form of Sodium Dodecyl Sulfate and Its Crystallization Process, ACS Omega, 6, 15770-15781, 10.1021/acsomega.1c01147, 2021.

Lei, T., Zuend, A., Cheng, Y., Su, H., Wang, W., and Ge, M.: Hygroscopicity of organic surrogate compounds from biomass burning and their effect on the efflorescence of ammonium sulfate in mixed aerosol particles, Atmos. Chem. Phys., 18, 1045-1064, 10.5194/acp-18-1045-2018, 2018.

Markarian, S. A., Harutyunyan, L. R., and Harutyunyan, R. S.: The Properties of Mixtures of Sodium Dodecylsulfate and Diethylsulfoxide in Water, Journal of Solution Chemistry, 34, 361-368, 10.1007/s10953-005-3056-x, 2005.

Moroi, Y., Motomura, K., and Matuura, R.: The critical micelle concentration of sodium dodecyl sulfate-bivalent metal dodecyl sulfate mixtures in aqueous solutions, Journal of Colloid and Interface Science, 46, 111-117, 10.1016/0021-9797(74)90030-7, 1974.

Umlong, I. M., and Ismail, K.: Micellization behaviour of sodium dodecyl sulfate in different electrolyte media, Colloids and Surfaces A: Physicochemical and Engineering Aspects, 299, 8-14, 10.1016/j.colsurfa.2006.11.010, 2007

Wiedensohler, A., Birmili, W., Nowak, A., Sonntag, A., Weinhold, K., Merkel, M., Wehner, B., Tuch, T., Pfeifer, S., Fiebig, M., Fjäraa, A. M., Asmi, E., Sellegri, K., Depuy, R., Venzac, H., Villani, P., Laj, P., Aalto, P., Ogren, J. A., Swietlicki, E., Williams, P., Roldin, P., Quincey, P., Hüglin, C., Fierz-Schmidhauser, R., Gysel, M., Weingartner, E., Riccobono, F., Santos, S., Grüning, C., Faloon, K., Beddows, D., Harrison, R., Monahan, C., Jennings, S. G., O'Dowd, C. D., Marinoni, A., Horn, H.-G., Keck, L., Jiang, J., Scheckman, J., McMurry, P. H., Deng, Z., Zhao, C. S., Moerman, M., Henzing, B., de Leeuw, G., Löschau, G., and Bastian, S.: Mobility particle size spectrometers: harmonization of technical standards and data structure to facilitate high quality long-term observations of atmospheric particle number size distributions, Atmos. Meas. Tech., 5, 657–685, https://doi.org/10.5194/amt-5-657-2012, 2012.

Wu, Junteng, Nicolas Brun, Juan Miguel González-Sánchez, et al. 2022. « Substantial Organic Impurities at the Surface of Synthetic Ammonium Sulfate Particles ». Atmospheric Measurement Techniques 15 (12): 3859-74. https://doi.org/10.5194/amt-15-3859-2022.